International Journal of Advance Research in Science and Engineering
Volume No.07, Special Issue No.03, April 2018
www.ijarse.com
IJARSE
ISSN: 2319-8354

DISCRIMINATION OF PAPILLARY AND MEDULLARY CARCINOMAS OF THYROID NODULES USING STATISTICAL FEATURES DRIVEN SUPPORT VECTOR MACHINE CLASSIFIER

B.Gopinath[1], R.Santhi[2]

[1]*Department of Electronics and Communication Engineering, Madanapalle Institute of Technology & Science, Madanapalle, Andhra Pradesh, India*

[2]*Department of Biochemistry, PSG College of Arts & Science, Coimbatore, Tamilnadu, India*

ABSTRACT

In this work, discrimination of two major types of carcinomas of thyroid nodule, namely, papillary and medullary carcinomas is addressed. The region based watershed segmentation technique is initially utilized to segment the medullary and papillary carcinoma cell regions in multi-stained Thyroid Fine Needle Aspiration Biopsy (FNAB) cytological images. It removes the background stain information from the images and retains the required foreground malignant cell information. Second order statistical features are, then, extracted from the segmented images using two-level Discrete Wavelet Transform (DWT) decomposition. The significant statistical features are used as meaningful descriptors by the Support Vector Machine (SVM) classifier for discriminating papillary and medullary carcinomas of thyroid nodules. The support vector machine classifier results highest promising discrimination accuracy of 95%. Also, the developed automated thyroid cancer diagnostic system produces 90% of sensitivity and 100% of specificity with respect to papillary and medullary thyroid carcinoma images.

Keywords: *Carcinoma, Discrimination, Malignancy, Segmentation, Thyroid, Watershed*

1. INTRODUCTION

Thyroid is one of the largest glands in the human body that regulates the rate of metabolism by producing thyroid hormones. The unwanted growth of cells around the thyroid gland can form a mass of tissue that is called as thyroid nodules. Most of these thyroid nodules are benign and not cancerous. About 5-10% of thyroid nodules are identified as thyroid malignant tumors and hence thyroid cancer is the most common endocrine malignancy and comprises 1-3% of all cancers [1]. The diagnosis of thyroid disorders is being carried out with Magnetic Resonance Imaging (MRI), Computed Tomography (CT), radioiodine scintigraphy and Positron Emission Tomography (PET) scanning, as well as Ultrasound (US) [2]. Fine needle aspiration biopsy (FNAB) is

a diagnostic test used for finding the risk of malignancy in the evaluation of thyroid nodule. Furthermore, FNAB is a minimally invasive procedure with low risks and can be usually performed by experienced physicians [3]. Thyroid FNAB deals with study of microscopic cytological images of thyroid nodules and is used as a screening tool to detect benign and malignant nature by studying the cytological features of cell structures. In this manual screening, thyroid biopsy sample derived from the patients are placed under a microscope in the form of smears in glass slides. And, a trained pathologist studies the cell structures and gives a diagnostic report. This manual screening procedure is, in few cases, subjective and may result misdiagnosis.

To overcome the misdiagnosis problem and improve the effectiveness of the diagnosis, efficient automated diagnostic systems are being developed for classifying benign and malignant states using image processing techniques. Thyroid nodule classification in ultrasound images was performed by fine-tuning deep convolutional neural network and a diagnostic accuracy of 96.34% was achieved [4].

The application of Learning Vector Quantization (LVQ) neural networks was investigated by Karakitsos et al. [5] for discriminating benign and malignant thyroid nodules and a diagnosis accuracy of 97.8% was reported for thyroid images stained by May-Grunwald-Giemsa staining protocol. Daskalakis et al. [6] designed a multi-classifier system for discriminating benign from malignant thyroid nodules using routinely H&E stained cytological images. It classified thyroid nodules using H&E stained FNAB cytological images and classification accuracy of 89.6% and 95.7% were reported for probabilistic neural network (PNN) single classifier and fusion of classifiers respectively. Gopinath et al. [7] conducted an experiment with ENN classifier trained by Gabor filter based features which reported a highest discrimination accuracy of 93.33%. In the previous work, Gopinath et al. [8] also experimentally tested decision tree, k-NN, ENN and SVM classifiers among which the ENN and SVM classifiers exhibited superior diagnostic accuracy of 90% to recognize benign and malignant thyroid nodules using the statistical textural features derived by two-level wavelet decomposition. The improved diagnostic accuracy of 96.66% achieved for the multiple classifiers with majority voting of k-NN, ENN and SVM classifiers and linear combination of single classifiers.

The conventional automated discrimination systems, in the literature, are normally developed for discriminating benign and malignant types of thyroid nodules. The proposed research work deals with the discrimination of two major types of thyroid carcinomas, namely, papillary and medullary carcinomas so that the pathologist can use the automated system for producing the diagnostic report with a specific type of thyroid carcinoma of the patients. In the development process, segmentation of foreground thyroid cancer cells in FNAB microscopic images of papillary carcinoma and medullary carcinoma of thyroid nodules are extracted with the help watershed transform method. Then, statistical textural features are extracted using two-level discrete wavelet transform decomposition and discrimination of cancer cells is performed by SVM classifier. Thus, this research work focuses on automatic discrimination of type of malignant carcinoma in Thyroid FNAB microscopic images.

The introduction of fine needle aspiration biopsy and thyroid carcinoma types are summarised in Section II. The region based watershed transform based segmentation method is described in Section III. Section IV describes the two-level wavelet decomposition of images for statistical feature extraction. The classification model using support vector machine is presented in Section V. Finally, the results and conclusion are presented in Sections VI and VII respectively.

2. THYROID CARCINOMA AND FINE NEEDLE ASPIRATION BIOPSY PROCEDURE

2.1 Thyroid Carcinoma

A type of cancer arising in the epithelial tissue of the thyroid gland is called thyroid carcinoma. Figure 1 summarizes various types of thyroid carcinoma. The thyroid malignancy originates either in the follicular or parafollicular cells. When it originates in the follicular cells, it either occurs as a differentiated or an undifferentiated tumor. When it is a differentiated tumor, it is either a Papillary Thyroid Carcinoma (PTC) which is around 70% of all thyroid malignancies) or a Follicular Thyroid Carcinoma (FTC) which is around 10-20% of all thyroid malignancies. Undifferentiated cancer or Anaplastic Thyroid Carcinoma (ATC) arising from the follicular cells is a highly aggressive carcinoma (1-2% of all thyroid malignancies). Malignant tumors also arise from the parafollicular cells or C-cells in the form of Medullary Thyroid Carcinoma (MTC) which is a rare type of carcinoma of the thyroid (3-5% of all thyroid malignancies) [9-11].

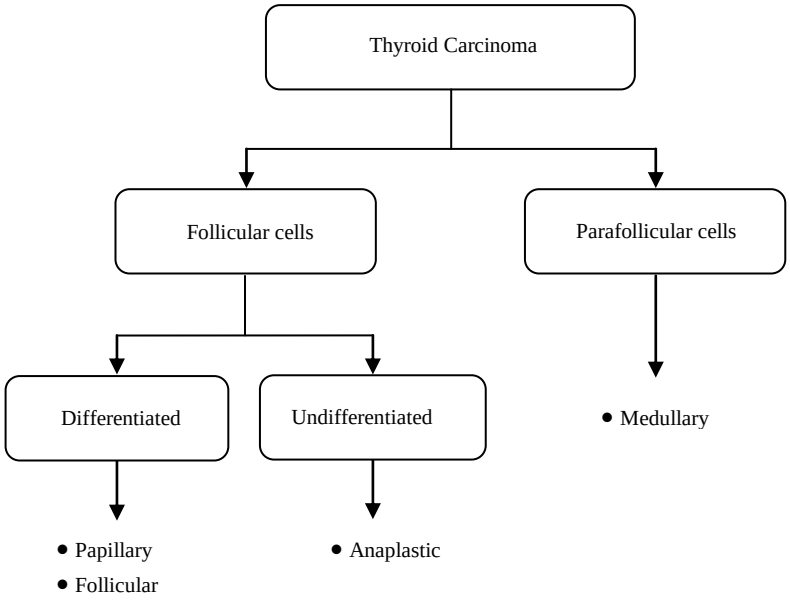

Fig. 1 Types of Thyroid carcinoma

2.2 Papillary carcinoma

About 80% of thyroid cancers are well-differentiated papillary carcinomas. Usually, they develop in only one lobe of the thyroid gland, but sometimes they occur in both lobes. Even though they grow slowly, papillary carcinomas often spread to the lymph nodes in the neck. A recent study has found that the survival rate of PTC at one year to be 97.5%, while the survival rate at 5, 10 and 15 to 20 years is 92.8%, 89.5% and 83.9% respectively, but most of the time, this can be successfully treated. The main diagnostic features of PTC are its nuclear changes, which include subtle irregularities in the nuclear contour and size, deep nuclear grooves and pseudo inclusions resulting from cytoplasmic invaginations. These nuclear features enable the diagnosis of PTC to be made on cytological examination and frozen section [11].

2.3 Medullary Thyroid Carcinoma

Medullary thyroid carcinoma accounts for about 5% of thyroid cancers. It arises from the calcitonin-producing parafollicular C-cells of the thyroid gland. Calcitonin is a hormone that helps to control the amount of calcium in blood. Carcinoembryonic antigen is a protein made by certain cancers, such as colorectal cancer and MTC. Because medullary cancer does not absorb or take up radioactive iodine, which is used for treatment, the prognosis is not quite as good as that for differentiated thyroid cancers [12].

The main diagnostic features of PTC are that the aspirates are usually highly cellular. However, scant cellularity is encountered with carcinomas containing extensive amyloid deposits and calcification. Tumor cells are predominantly single cells, but can also be seen as sheets, loose clusters, syncytia, rosettes, cords, and papillae. The cells are usually uniform in size and shape but occasionally can present as large pleomorphic cells. Nuclei are eccentrically placed, giving the cells a plasmacytoid appearance, and binucleation and multinucleation are common. Nuclei have a coarsely granular chromatin texture and inconspicuous nucleoli [13].

Figure 2 shows the sample FNAB cytological microscopic images of papillary carcinoma and medullary carcinoma of thyroid nodules. Fig. 2(a) shows a papillary carcinoma image with numerous nuclear grooves and Fig. 2(b) shows a medullary carcinoma image with relatively monomorphic fusiform cells and amyloid.

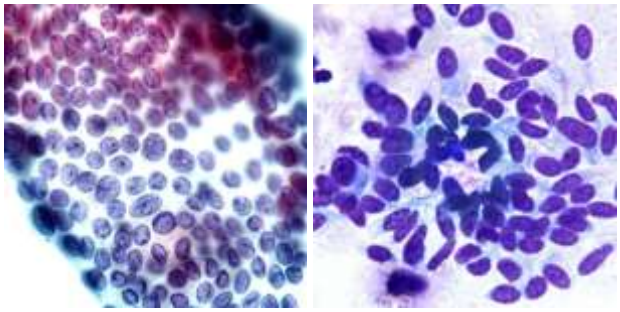

(a) (b)

Fig. 2(a) Papillary carcinoma image with numerous nuclear grooves and Fig. 2(b) Medullary carcinoma image with relatively monomorphic fusiform cells and amyloid.

2.4 Fine Needle Aspiration Biopsy Procedure

Fine Needle Aspiration Biopsy is a simple and safe method of determining benign or malignant state of the thyroid nodule. Initially, thyroid biopsy samples from the thyroid nodule of a patient are extracted using a 25 gauge needle with disposable 10cc syringe and sent to the pathology laboratory. The pathologist prepares smears in glass slides and examines cell structure of the sample under a microscope based on the cytological features. After examining all the slides, the pathologist prepares a cytological diagnosis report. The diagnosis report classifies the samples as benign, malignant, suspicious or inadequate. If it is malignant, type of the carcinoma can also be diagnosed. Normally, the accuracy of FNAB technique is around 95%, and false negative and false positive results vary from 0-5% [14].

To automate this manual process and develop an automated diagnostic system, the cytological images are captured by attaching a digital camera with microscope and these images can be processed using image

processing techniques. The parameters sensitivity, specificity and discrimination accuracy can be derived for the assessment of thyroid malignancy in terms of True Positive (TP), False Positive (FP), True Negative (TN) and False Negative (FN). True positive is a positive result in the FNAB for malignancy and confirmed in the cytological study. False positive is a positive result for malignancy but not confirmed in the study. True negative is a negative result for malignancy and no carcinoma in the study. False negative is a negative result for malignancy but with a carcinoma in the study. Sensitivity (S) can be defined as the proportion of patients with associated carcinoma and a positive result in the FNAB for malignancy (1). Specificity (Sp) can be defined as proportion of patients without associated carcinoma and with a negative result in the FNAB for malignancy (2). The Discrimination Accuracy (DA) can be derived as the proportion of patients diagnosed correctly by the diagnostic test (3).

$$S = TP/(TP + FN) \quad (1)$$

$$Sp = TN/(TN + FP) \quad (2)$$

$$DA = (TP + TN)/(FP + FN + TP + TN) \quad (3)$$

Figure 3 shows various stages involved in the development of an automated diagnosis system that include segmentation, feature extraction and classification stages.

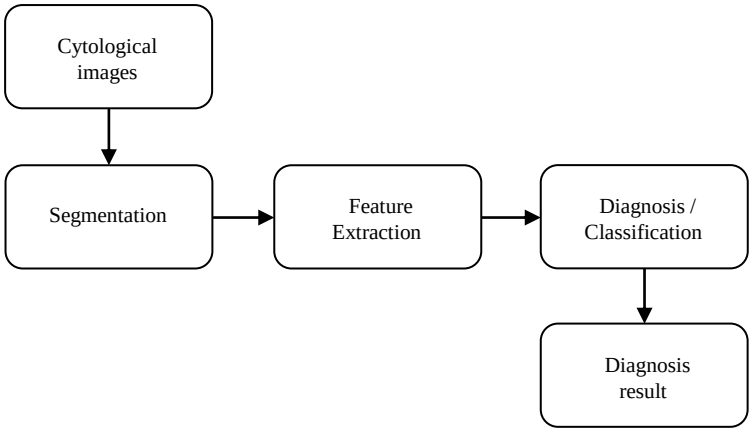

Fig. 3 Various stages of an automated cancer diagnostic system

The thyroid FNAB images shown in Fig. 2 are stained by various types of stains. The discrimination accuracy of the diagnostic system will be affected by the background stain pixels and hence removal of the unwanted background pixels from the images is required by using an appropriate segmentation method. The feature extraction stage is used to extract the significant second order statistical feature vectors from the segmented images and these features are used as useful descriptors for describing the cytological characteristics of papillary and medullary carcinoma types. The statistical feature vectors drive the third and final stage of classification with support vector classifier as a decision making tool.

3. WATERSHED IMAGE SEGMENTATION

The discrimination accuracy of the proposed work purely depends on the efficient segmentation methodology and corresponding foreground cell structure information. In this work, Euclidean distance transform based

watershed transform is implemented to segment the required cancer cell regions of medullary and papillary carcinomas in multi-stained FNAB images.

The flow diagram of the watershed transform segmentation method is shown in Fig. 4. The initial pre-processing step is performed on the malignant images to convert color image into gray scale image and separate foreground pixels from the background pixels using Otsu's thresholding technique based on the different intensities of the pixels. According to Otsu's method, an appropriate threshold value is calculated. Each pixel in the image is compared with the threshold value. When the pixel's intensity is higher than this threshold value, the pixel is set to white while it is less than the threshold value, it is set to black in the output image [15]. The input to the thresholding operation is a gray scale image and the output is a binary image. Thus, the black and white pixels related to background and foreground information of the malignant images are separated.

The thresholded images are then fed to watershed segmentation algorithm in association with distance transform. The distance transform provides a measure of the separation of points in the image that calculates the distance between each pixel that is set to zero and the nearest nonzero pixel. The distance transform is normally applied to binary images. However, the result of the transform is a gray scale image that looks similar to the input image. But the gray level intensities of foreground regions are changed to show the distance to the closest boundary from each point. In this work, Euclidean distance metric is used because it is similar to the measurement of the objects in the real world. Euclidean distance calculates the root of square differences between coordinates of a pair of objects. The Euclidean distance D between two pixels in a binary image, (x_1, y_1) and (x_2, y_2), is calculated as given in (4):

$$D = \sqrt{(x_1 - x_2)^2 + (y_1 - y_2)^2} \qquad (4)$$

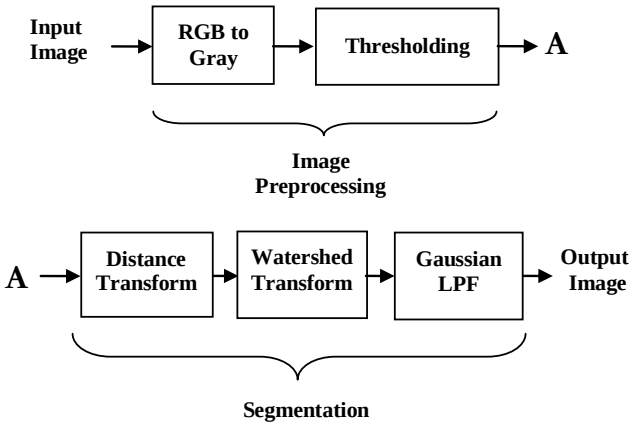

Fig. 4 Watershed segmentation method

The watershed transform is a region based segmentation technique in which the images are treated as topographic surface and the intensity values of the images are considered as heights. If a topographic surface is flooded by water, then a watershed is being the dividing line between the domains of attraction of rain falling over the region [16]. The watershed transform applies this idea to process the gray scale images to perform the segmentation operation. Thus, catchment basins are treated as regions in the gray scale image and watersheds are being as the lines dividing the regions. The input papillary and medullary carcinoma images are converted into binary images so that the distance transform can be applied. The distance transform converts them into gray

scale images so that catchment basins are identified as regions and then watersheds are found by converting the images into complement images.

The main disadvantage of watershed segmentation is over segmentation of the image because of many small basins and watershed lines. This over segmentation problem can be solved by using a suitable Low Pass Filter (LPF) in conjunction with the output of watershed transform. In this work, a Gaussian LPF is generated with a *5x5* Gaussian kernel and convolved with the output image of watershed transform to remove the unwanted noise pixels generated due to over segmentation.

4. FEATURE EXTRACTION USING WAVELET DECOMPOSITION

In this work, two-level Discrete Wavelet Transform (DWT) decomposition is implemented for extracting second order statistical features from the segmented image sets of papillary and medullary thyroid carcinoma images [17].

In two-level DWT decomposition, the malignant images are initially divided into four sub-bands namely LL1, LH1, HL1 and HH1 using separable filters and LL1 band is further divided into LL2, LH2, HL2 and HH2. The LL2 band can be used for further decomposition based on the requirement. The representation of two-level decomposition is shown in Fig. 5.

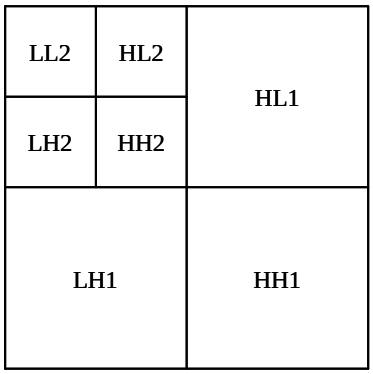

Fig. 5 Two-level Wavelet Decomposition

A total of eight second order statistical features, namely, mean, standard deviation, entropy, variance, energy, homogeneity, contrast and correlation are extracted and stored in feature database as listed in Table 1.

Table 1. Eight second order statistical features

Statistical Feature	Description
Mean	$\sum_{i,j} f(i,j)/N$
Standard Deviation	$\sum_{i,j} ((f(i,j)-\mu)^2/N)^{\frac{1}{2}}$
Entropy	$-\sum_{i,j} f(i,j)\ log\ f(i,j)$
Variance	σ^2
Energy	$\sum_{i,j} f(i,j)^2$

Statistical Feature	Description
Homogeneity	$\sum_{i,j} \frac{f(i,j)}{1+\lvert i-j\rvert}$
Contrast	$\sum_{i,j} f(i,j)\,(i-j)^2$
Correlation	$\sum_{i,j} f(i,j)\,(i-\mu_i)\,(j-\mu_j)/\sigma_i\sigma_j$

where, $f(i,j)$ is the gray-level value for each pixel in the region of interest, N is the total number of pixels in the region of interest and μ_i, μ_j, σ_i, σ_j, σ_j^2 are means and standard deviations of $f(i,j)$.

A total of 30 thyroid carcinoma slide images with a combination of 15 papillary and 15 medullary carcinoma images are collected for conducting the study. Since the size of the image set is small, each image is auto-cropped into four images so that the total number of images becomes 120 among which 60 are papillary carcinoma images and remaining 60 are medullary carcinoma images.

Now, 50 papillary carcinoma images and 50 medullary carcinoma images are combined together for training set and 10 papillary carcinoma images and 10 medullary carcinoma images are combined together for testing set. During the feature extraction phase, a total of eight statistical features are derived from each image and hence the total number of features derived from training and testing set images become 480 and 160 respectively as summarized in Table 2. In this work, image size is resized and maintained as 256x256 for original slide images and they are equally cropped into four 128x128 images. For conducting the current study, the thyroid FNAB images have been collected from on-line image atlas of Papanicolaou Society of Cytopathology which are reviewed and approved by the atlas committee [18].

Table 2. Grouping of images for training and testing set

Images / Features	Training Set	Testing Set
Number of slide images	15	5
Number of cropped images	60	20
Number of statistical features from each image	8	8
Total number of statistical features	480	160

The best feature vectors with high significant levels are selected from the distribution of these features by calculating median values of all the features for papillary and medullary groups and tabulated in Table 3. From Table 3, it is observed that the difference in median values is significant for the features mean, standard deviation, variance and energy and hence there is a possibility of differentiating between papillary and medullary feature sets of thyroid FNAB images using these features. For the remaining features contrast, homogeneity, entropy and correlation, the difference in median values is lesser than one these features exhibit no significant difference between papillary and medullary carcinoma feature sets. Thus, it is concluded that the features mean, standard deviation, variance and energy are having significant impact in the discrimination process compared with the remaining features contrast, homogeneity, entropy and correlation.

Table 3. Median values of feature vectors derived from segmented thyroid carcinoma images

Statistical Features	Median Value		Difference in Median Value between two groups
	Papillary Group	Medullary Group	
Mean	10.52×10^{6}	12.91×10^{6}	2.39
Standard Deviation	14.18×10^{6}	16.12×10^{6}	1.94
Variance	1.87×10^{14}	2.99×10^{14}	1.12
Energy	1.15×10^{12}	2.33×10^{12}	1.18
Contrast	16.24×10^{3}	16.30×10^{3}	0.06
Homogeneity	29.22×10^{-3}	29.32×10^{-3}	0.1
Entropy	885.1×10^{-3}	884.8×10^{-3}	0.3
Correlation	0.54×10^{-3}	0.56×10^{-3}	0.02

5. DISCRIMINATION OF MALIGNANCIES

In any supervised classification, two steps are followed, namely, training step and testing step. In training step, the labeled papillary and medullary carcinomas training image set are segmented and statistical features are extracted using discrete wavelet transform and stored in feature library. In the testing step, the discrete wavelet transform is again applied on the unlabeled and segmented test set images of papillary and medullary carcinomas. The second order and similar set of statistical features are extracted and used for discrimination using support vector classifier as illustrated in Fig. 6. The SVM classifier performs the machine learning based on the principle of structural risk minimization (SRM). The concept of SRM is to maximize the margin between a separating hyper plane and closest data points as shown in Fig. 6. A separating hyperplane refers to a plane in a multi-separating hyperplane that maximizes the margin from closest data points to the plane.

The SVM classifier is a highly efficient kernel based classifier which maps the given statistical feature patterns into a higher dimensional space. It constructs a decision hyperplane in this higher dimensional space. The feature vectors lying on the hyperplane margins are called as support vectors. And each feature pattern is then classified by assigning a decision value which is the perpendicular distance to the hyperplane. By convention, the origin of the feature space is shifted to lie on the hyperplane, giving positive and negative decision values so that sign indicates the predicted class [19].

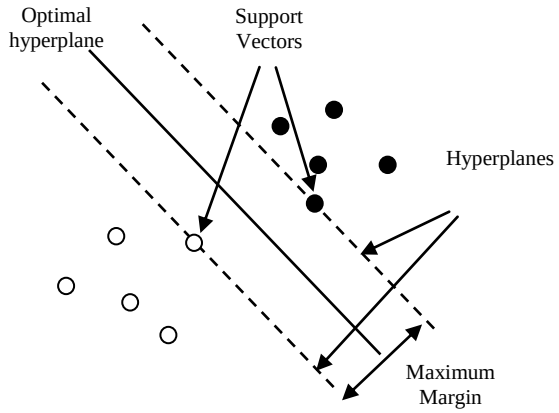

Fig. 6 Components of support vector machine

6. RESULT AND DISCUSSION

The performance of the proposed discrimination model based on SVM classification model tested with the statistical features derived from two-level discrete wavelet decomposition is presented in Table 4. From the discrimination results, the best performance is achieved by incorporating the statistical second order features derived from FNAB images segmented by watershed segmentation method with 95% of discrimination accuracy, 90% of sensitivity and 100% of specificity. Normally, in a conventional automated discrimination systems, discrimination of benign and malignant types of thyroid nodules are being carried out. Karakitsos *et al.* investigated the use of neural networks to discriminate benign and malignant thyroid lesions and achieved 97.8% of diagnostic accuracy using thyroid FNAB images stained by MGG staining protocol [5]. Daskalakis *et al.* designed a multi-classifier system for discriminating benign from malignant thyroid nodules using H&E stained FNAB cytological images and diagnostic accuracies of 89.6% and 95.7% were reported for PNN single classifier and combined classifiers respectively [6]. These studies were not dealing with multi-stained FNAB images. Our previous study [7] with multi-stained and auto-cropped thyroid FNAB images demonstrated a reasonable diagnostic accuracy of 90% using ENN and SVM classification models. Similarly, our study achieved a promising diagnostic accuracy of 96.66% with multi-stained and auto-cropped thyroid FNAB images using majority voting and linear combination rules based multiple classifier fusion [8]. But, in the proposed research work, discrimination of two major types of thyroid carcinomas, namely, papillary and medullary carcinomas has been performed so that the pathologist can use the automated system for producing the diagnostic report with a specific type of thyroid carcinoma of the patients.

Table 4. Performance comparison with existing works

Research Works	Nature of work	Classifiers	Discrimination accuracy
Karakitsos et al. [5]	Discrimination of benign from malignant thyroid lesions	LVQ-NN	97.8%
Daskalakis et al. [6]	Discrimination of benign from malignant thyroid nodules	PNN	89.6%
		k-NN/PNN/ Bayesian	95.7%

Gopinath et al. [7]	Discrimination of benign from malignant thyroid nodules	*k*-NN	70%
		SVM	90%
		ENN	90%
Gopinath et al. [8]	Discrimination of benign from malignant thyroid nodules	Multi-classifier	96.66%
Proposed Work	Discrimination of type of thyroid malignancy	SVM	95%

7. CONCLUSION

Discrimination of Papillary and Medullary carcinoma malignancy in thyroid FNAB cytological images was presented using support vector machine classifier with a help of region based watershed segmentation method as a preprocessing step. The performance analysis of the discrimination system was measured in terms of discrimination accuracy, sensitivity and specificity. The discrimination accuracy of 95% is achieved with the combination of watershed segmentation and discrete wavelet features with 90% of sensitivity and 100% of specificity. This research work attempted to perform multi-class discrimination problem with respect to papillary and medullary thyroid carcinoma images. When the conventional discrimination process performs the classification of benign and malignant states of thyroid nodules, the propose work can aim to further discriminate type of the malignancy for the malignant result. Hence, the proposed automated diagnostic system can help the pathologists as a second opinion tool.

REFERENCES

[1]. R.L. Siegel, K.D. Miller, and A. Jemal, Cancer statistics, *CA: A Cancer Journal for Clinicians, 65(1)*, 2015, 5-29.

[2]. C.A. Meier, *Role of Imaging in Thyroid Disease*, In: J. Hodler, G.K. Von Schulthess, C.L. Zollikofer (eds), Diseases of the Brain, Head & Neck, Spine, Springer, Milano, 2008.

[3]. P. Locantore, F. Ianni, and A. Pontecorvi, *Fine Needle Aspiration Biopsy*, In: C. Lombardi, and R. Bellantone (eds), Minimally Invasive Therapies for Endocrine Neck Diseases, Springer, Cham, 2016.

[4]. J. Chi, E. Walia, P. Babyn, J. Wang, G. Groot, and M. Eramian, Thyroid Nodule Classification in Ultrasound Images by Fine-Tuning Deep Convolutional Neural Network, *Journal of Digit Imaging, 30(4)*, 2017, 477-486.

[5]. P. Karakitsos, B. Cochand-Priollet, A. Pouliakis, P.J. Guillausseau, and A. Ioakim-Liossi, Learning vector quantizer in the investigation of thyroid lesions, *Analytical and Quantitative Cytology and Histology, 21*, 1999, 201-208.

[6]. Daskalakis, S. Kostopoulos, P. Spyridonos, D. Glotsos, P. Ravazoula, M. Kardari, I. Kalatzis, D. Cavouras, and G. Nikiforidis, Design of a multi-classifier system for discriminating benign from malignant thyroid nodules using routinely H&E-stained cytological images, *Computers in Biology and Medicine, 38*, 2008, 196-203.

[7]. Gopinath, and N. Shanthi, Computer-aided diagnosis system for classifying benign and malignant thyroid nodules in multi-stained FNAB cytological images, *Australasian Physical & Engineering Sciences in Medicine, 36*, 2013, 219-230.

[8]. Gopinath, and N. Shanthi, Development of an Automated Medical Diagnosis System for Classifying Thyroid Tumor Cells using Multiple Classifier Fusion, *Technology in Cancer Research and Treatment, 14(5)*, 2015, 653-662..

[9]. H.J. Biersack, and F. Grunwald, *Thyroid Cancer*, Berlin: Springer Verlag, 2005.

[10]. Y.C. Oertel, *Classification of Thyroid Malignancies*, In: L. Wartofsky, D. Van Nostrand (eds), Thyroid Cancer: A Comprehensive Guide to Clinical Management, Human Press, New Jersey, 2004, 85-87.

[11]. C.M. Slough, and G.W. Randolph, Workup of well-differentiated thyroid carcinoma, *Cancer Control, 13(2)*, 2008, 99-105.

[12]. F. Pacini, M.G. Castagna, L. Brilli, and G. Pentheroudakis, Thyroid cancer: ESMO Clinical Practice Guidelines for diagnosis, treatment and follow-up, *Annals of Oncology, 21(5)*, 2010, 214-219.

[13]. A.J. Adeniran, and D. Chhieng, *Medullary Carcinoma*, In: Common Diagnostic Pitfalls in Thyroid Cytopathology, Springer, Cham, 2016.

[14]. S.A. Mahar, A. Husain, and N. Islam, Fine needle aspiration cytology of thyroid nodule: Diagnostic accuracy and pitfalls, *Journal of Ayub Medical College, 18(4)*, 2006, 26-29.

[15]. N. Otsu, A threshold selection method from gray-level histograms, *IEEE Transactions on Systems, Man, and Cybernetics, 9*, 1979, 62-66.

[16]. K. Nallaperumal, K. Krishnaveni , J. Varghese, S. Saudia , S. Annam, and P. Kumar, A novel Multi-scale Morphological Watershed Segmentation Algorithm, *International Journal of Imaging Science and Engineering, 1(2)*, 2007, 60-64.

[17]. S. Arivazhagan, and L. Ganesan, Texture Classification using Wavelet Transform, *Pattern Recognition Letters, 24(9-10)*, 2003, 1513-1521.

[18]. http://www.papsociety.org/atlas.html

[19]. M.S. Kavitha, A. Asano, A. Taguchi, T. Kurita, and M. Sanada, Diagnosis of osteoporosis from dental panoramic radiographs using the support vector machine method in a computer-aided system, *BMC Medical Imaging, 12(1)*, 2012.